



**HAL**  
open science

## Visual Analysis of Urban Environment

François Sarradin, Daniel Siret, Gérard Hégron

► **To cite this version:**

François Sarradin, Daniel Siret, Gérard Hégron. Visual Analysis of Urban Environment. First International Workshop on Architectural and Urban Ambient Environment, Feb 2002, Nantes, France. halshs-02472303

**HAL Id: halshs-02472303**

**<https://shs.hal.science/halshs-02472303>**

Submitted on 10 Feb 2020

**HAL** is a multi-disciplinary open access archive for the deposit and dissemination of scientific research documents, whether they are published or not. The documents may come from teaching and research institutions in France or abroad, or from public or private research centers.

L'archive ouverte pluridisciplinaire **HAL**, est destinée au dépôt et à la diffusion de documents scientifiques de niveau recherche, publiés ou non, émanant des établissements d'enseignement et de recherche français ou étrangers, des laboratoires publics ou privés.

# **Visual Analysis of Urban Environment**

François Sarradin — Daniel Siret — Gérard Hégron

Laboratoire CERMA – École d'Architecture de Nantes

Rue Massenet – BP 81 931

44 319 NANTES CEDEX 3

{sarradin,siret,hegron}@cerma.archi.fr

## **1. Introduction**

This paper presents a survey of methods used to model and to analyse visual events in urban scenes. What we call a visual event is an event which occurs in the visual field while we are moving or while the scene is moving. This could be an object appearance or disappearance, or a shape, a colour, or a texture modification. But here, we mainly consider the visual events provided by objects set during a motion.

In the second section, we examine some methods to model the events that come inside our visual field, giving a first interpretation to a urban environment. This is done after showing methods to represent the visual field. In the third section, we focus on different methods used to analyse and to evaluate the visibility in urban environment. Finally, we conclude on the way each of these representations of visual perceptions and each of these visual analysis methods act, and in which way they could be extended.

## **2. Visual event representation**

Representation of urban scenes can be made by symbolizing buildings, streets, places, etc. We can also add the visual events which appear as observers move in the streets. The visual events generate transitions in the observer visual field like appearance and disappearance of objects, colour changing, shape transformation, etc. They provide important information about the visual effects.

The purpose of this section is about the representation of visual events. First, we show 2D motionless projections of the visual field which can be used in this representation. Second, we present the visual event sequences acting by motion decomposition into pictures. Apart from all projection, Lynch and Thiel proposed a notation to describe the visual perception of space and motion, and the orientation sense. Then, we show 2D and 3D methods to determine visual events and regions where visual informations do not change.

### ***2.1. 2D projections of the visual field***

Here, we study the visual field representations in a motionlessness context. Most of these representations use a geometrical projection in order to imitate what we see or how we record our visual world.

#### ***2.1.1. Perspective projection***

The perspective projection study began with italian painters from Renaissance. They wished to create an illusion: their goal was to show objects in three dimensions inside their paintings. It is used in architecture or in image synthesis in order to give a realistic representation. It is also used in simulation for architectural and urban project in order to determine the sun lighting time or the incident energy from the sky [Groleau, 2002].

According to Panofsky, the perspective projection is “the aptitude to represent several

objects with the part of the space in which they are, so that the concept of material support of the picture is completely driven out by the concept of transparent plan, so that we believe, our glance crosses to plunge into an imaginary external space which would contain all these objects into an apparent succession and which would not be limited but only cut out by the edges of the picture” [Panofsky, 1975].

The main concept in perspective is this notion of transparent plan where the image of the scene is projected. Teller brings a definition to explain the perspective projection principles (Figure 1):

“[...] The perspective projection method is defined as the intersection between the visual lines which link observer eye to points of the real world, and a plane staying at a distance  $D$  from observer eye and perpendicular to the vision direction.” [Teller, 2001]

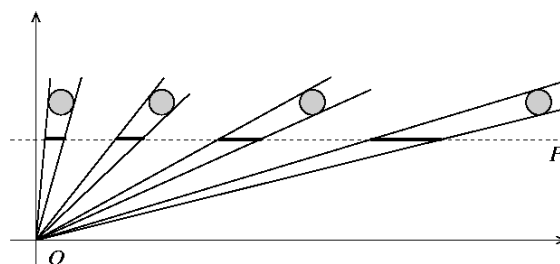


Figure 1: Perspective projection for the same object at different distances.

However, Panofsky notices that the perspective representation involves two assumptions: on the one hand, a unique and motionless eye generates our vision; on the other hand, the intersection plane is an appropriate picture of our visual field [Teller, 2001]. In fact, the perspective representation is near the retinal image for a sufficient vision angle interval. But, as the retina is curved and not flattened, the perspective projection differs from retinal image for a wide vision angle. Another disadvantage is that the perspective projection is not consistent with the eighth Euclid’s theorem which states that the visible difference between two identical objects unequally spaced must not be determined by their respective distance, but by their visual angles [Teller, 2001]. On the Figure 1, we can notice the deformation produced by the perspective projection. The observer stands on  $O$  point and his eyes is directed to the top of the page;  $P$  is the image plane of the perspective projection. For the observer the outer object appears wider than the closer one. This deformation is due to the fact that the perspective projection cuts linearly the solid angle of each object (this is known as the *Leonardo’s Paradox* [Weisstein, 1999]).

Thus, the perspective projection can be assimilated to the retinal image for small observation angles. However, it is not adapted for visual field representation with wide angle, which is useful to anticipate on what we will see.

A particular case of the perspective projection is used in architecture and called *axonometry*. This projection consists in setting the observer to infinite distance so that visual lines are parallel. As a result, the axonometry preserves neither area nor angle but only distance. It is often used for solar simulation purposes — the sun is supposed to be at the infinite.

### 2.1.2. Spherical projection

The spherical projection is used in cartography for Earth representation. Thiel used it for representing luminous sources in its notation [Thiel, 1969], and the LEMA for solar access decision-making [Teller and Azar, 2001]. In order to analyse urban scenes, Teller worked

with three kinds of spherical projections.

The spherical projection can be defined as the intersection between visual lines, which link observer eye to points of the real world, and a sphere centred at observer eye. It allows a visual world representation in all directions at a time (above, below, in front, etc.) This panoramic representation is closed to our perception of the visual world which is composed by a snapshot series of our visual field [Dupagne *et al.*, 1997]. As this snapshot is senseless, our visual world image is persistent and stable (see [Gibson, 1950]). Unlike perspective projection, all dimensions depend on distance to the observer [Teller, 2001]. It comes from the fact that the spherical projection acts by cutting the solid angles of objects with a sphere. Suppose that the projection is made on a sphere which radius is 1; then, the projection function is (Figure 2) :

$$M(x, y, z) \mapsto M' \left( \frac{x}{D_M}, \frac{y}{D_M}, \frac{z}{D_M} \right)$$

Where  $D_M = \sqrt{x^2 + y^2 + z^2}$  is the distance between the observer and the point  $M$  which coordinates are  $(x, y, z)$ .

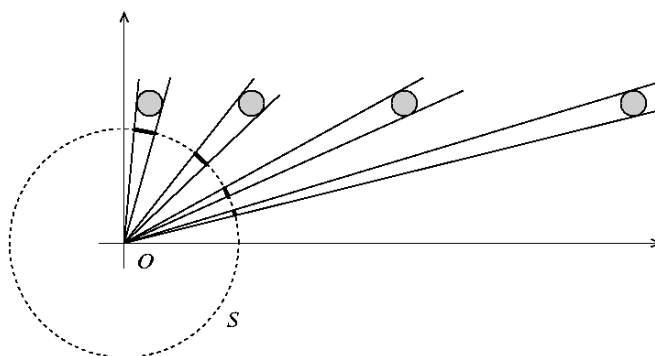


**Figure 2: Spherical projection for the same object at different distances.**

However, a spherical projection is a three-dimensional representation and it is not directly exploitable. It is necessary to apply another transformation that projects the spherical image on a plane. There are several kinds of transformations to flatten the sphere. Their deformations provide to spherical projection specific characteristics which allows to adapt spherical projection for particular cases.

For urban morphology study, Teller works around three flattening functions shown in Figure 3.

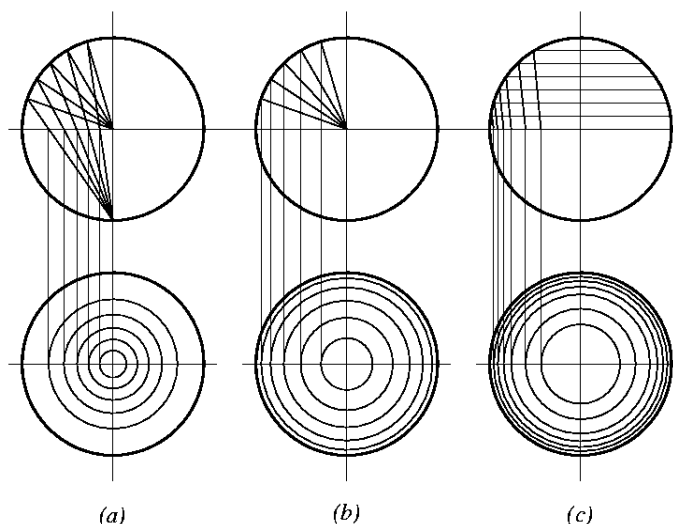


Figure 3: Three transformations to flatten a sphere [Teller, 2001]: (a) stereographic projection, (b) orthogonal projection, (c) isoaire projection.

- *Stereographic projection* (Figure 4). The stereographic projection is a “map projection in which great circles are circles and loxodromes<sup>1</sup> are logarithmic spirals” [Weisstein, 1999]. Its main property is to conserve tangential angles. According to Teller, the stereographic projection preserves visual aspect of 3D shapes rather well [Teller, 2001]. The flattening function is given below [Teller and Azar, 2001]:

$$(x, y, z) \mapsto \left( \frac{x}{1+z}, \frac{y}{1+z} \right)$$

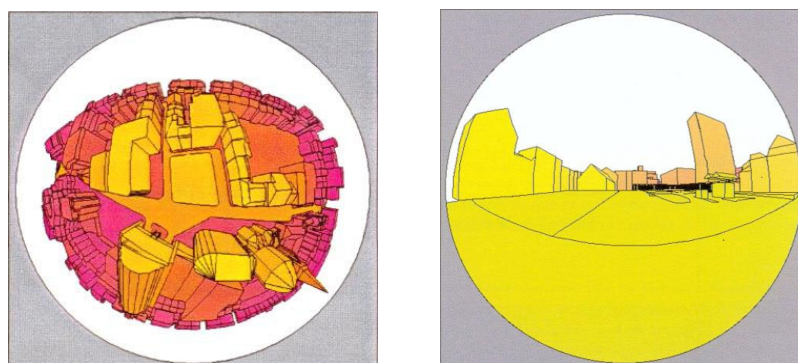


Figure 4: Stereographic projection in Liège (right: place Xavier-Neujean [Teller, 2001], left: Cité administrative [Dupagne *et al.*, 1997]).

- *Orthogonal projection*. The orthogonal projection preserves the vertical angles. Thus, the radial distances inside the projection is proportional to the observable height. However, it does not preserve neither area nor angle. The equidistant projection is useful to compare the visual height. Its flattening function acts by a substitution of the height [Teller and Azar, 2001]:

$$(x, y, z) \mapsto (x, y)$$

- *Isoaire projection*. With the isoaire projection, the surfaces projected on the image are representative of the solid angles intercepted on the sphere. The flattening function is given below [Teller and Azar, 2001]:

<sup>1</sup> “The loxodrome is the path taken when a compass is kept pointing in a constant direction” [Weisstein, 1999].

$$(x, y, z) \mapsto \left( \frac{x\sqrt{1-z}}{\sqrt{x^2+y^2}}, \frac{y\sqrt{1-z}}{\sqrt{x^2+y^2}} \right)$$

The spherical projection is an interesting representation of the visual world as it is relatively consistent with our representation. Although it can not be exploited directly, a map projection (i.e. stereographic projection, equidistant projection, isoaire projection) applied to the spherical projection produces deformations which highlight scene characteristics like height ratio, area shape ratio or angle ratio. From a certain viewpoint, the spherical projection is adaptable. However, it presupposes that we have a unique eye, and, as it is a projection on a surface, the deepness ratio between objects disappears. The projection of a small and near object can be as important as a bigger but farther one.

We will show in section 3.3 a use of spherical projection in visual analysis of urban scenes by processing sky opening generated by the building shapes.

## 2.2. Visual event sequences

A sequence is a series of more or less realistic images ordered in time, which is obtained during a motion (i.e. motion of the visual field, or motion of an object in the visual field). In order to decompose movement into image series, Eadweard Muybridge generated several photographic sequences, between 1884 and 1885, with an apparatus composed of several cameras linearly disposed. This strange apparatus was able to decompose human or animal motions (e.g. walking, running, jumping, etc.) Then, the Lumière's brothers created the *Cinématographe* in 1894. Its principle was to decompose movement into image sequences.

Much later, some urban designers have argued that movement can be read and understood as a pictorial sequence. Namely, Cullen talked about the approach of architectural objects by using pictorial sequences [Cullen, 1961]. Appleyard, Lynch *et al.* tried different techniques to record visual sequences in order to analyse it [Appleyard *et al.*, 1964]. One of them consists in using the motion pictures which record sequences in a permanent form that can be shown to large groups of people. However, they did not keep this technique because of “the inherent difference between the camera and the human eye” [Appleyard *et al.*, 1964]. Later, Bosselmann tried to represent a walk through Venice by using a sequence of drawings with a text explaining what he saw plus additional informations [Bosselmann, 1998]. However, the author noticed some disadvantages to this technique. For example, the glance direction in the drawings follows the observer motion direction. Besides, there are no drawing representing the view to the right, to the left, at rear, etc. Thus, no drawing could represent the view which opens on each side of the observer when he is on a bridge for example [Bosselmann, 1998].

In this section, we will focus on a method, proposed by Panerai, based on pictorial sequences, which record the visual effects.

### *Sequential analysis*

In order to record the motion, the movie cameras decompose it into a series of image. Panerai reused this idea of visual sequence and adapted it to represent visual events on urban routes [Panerai, 1970][Panerai *et al.*, 1997, 1999]. Inspired by de Wolfe [de Wolfe, 1963], this method proceeds by isolating and identifying in a sequence different pictures which refer to a codified and schematic configuration of the scene. These pictures can be named [Panerai *et al.*, 1999]:

- Picture illustrating general viewpoints: symmetry or dissymmetry; lateral demarcation or axial demarcation; opening or closure; convexity or concavity.
- Pictures insisting on lateral walls: horizontal or vertical cutting up, undulation; face

relation; deference, indifference, or competition.

- Pictures studying lateral walls extension to vanish point and beyond: narrowing, strangling, or wings effect; open or hidden highlighting; deflection; demarcation.
- Pictures characterizing the front closure of the visual field: centring or diaphragm.

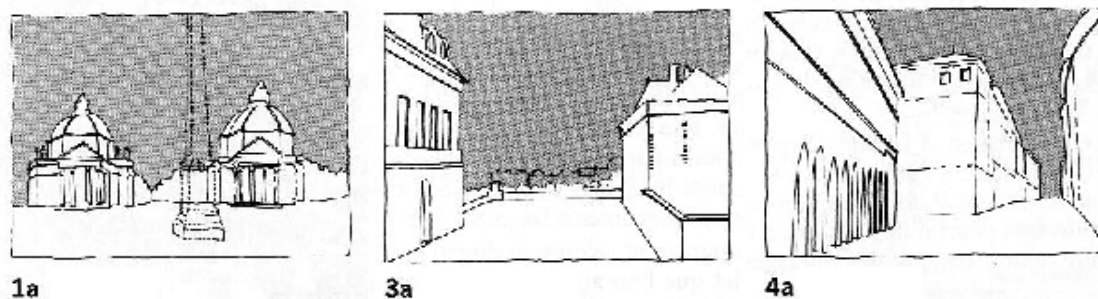


Figure 5: Examples of picturesque elements [Panerai *et al.*, 1999]: symmetry (1a), opening (3a), convexity (4a).

A sequence is composed of a particular picture suite configuration that can be called a *linkage*<sup>2</sup>. A picturesque scene results in accumulation in short distances of breaks in the logic of the linkage. For monumental effects, the sequence consists of relatively slow successions with superpositions of pictures.

In order to complete sequential analysis, it is necessary to collect pictures and linkages in order to get set of linkages and to process entire sequences. A first solution consists in assembling pictures linked to an object. In this case, landmarks and monuments play a primary role and sequences are generated by these objects. A second solution consists in assembling pictures by theme, then to introduce the cuts when the theme changes; a sign or a mark allows sometimes to determine a cut.

The sequential analysis method was tested by Dupagne and Teller, with pictures produced by stereographic projection, in order to study routes in open spaces [Dupagne *et al.*, 1997] (see section 2.1). Following their point of view, it is not really a tool for decision-making. They describe it as a basic tool to serve in reflection or in presentation of project intents.

### 2.3. Visual event notation

#### 2.3.1. The view from the road

As we walk in the street or drive on the road, we see all kind of visual informations which reveal our motion. They are based on our knowledge of architectural objects. In the United States, during 1950s, it is possible to drive on expressways through the cities at accelerated speed. On these quick axis, the visual informations are numerous and stream quickly. In answer to the confusion that could be generated by this evolution, Appleyard, Lynch and Myer have created a notation in a view to provide an ‘artistic’ sense for highway because: “road-watching is a delight, and the highway is — or at least might be — a work of art” [Appleyard *et al.*, 1964]. Their notation is based on notation used by Lynch in [Thiel, 1969] and by Thiel.

Two components are considered: the space and the motion sensations on the one hand, the observer orientation on the other hand. For the first one, Appleyard, Lynch and Myer have classified the visual informations relative to the motion type they involve [Appleyard *et al.*, 1964]. The motion sensation includes the apparent self-motion generated by the road (e.g.

<sup>2</sup> Panerai uses the french term *enchaînement* that could to be translated into the term ‘linkage’ used for cinema.

speed variation, direction variation, altitude variation, etc.) and the apparent motion of the visual field (e.g. deformations, rotations, translations, etc.) To this list, it should be appended spatial characteristics like light quality, space proportion, space transition, etc. An example of the notation corresponding to the motion and the space sensations is given in the left side of the Figure 6. The scheme represents an abstraction of a road which goes down to a turn with high lateral edges. At the end of the turn, the driver climbs and the view is opening [Appleyard *et al.*, 1964].

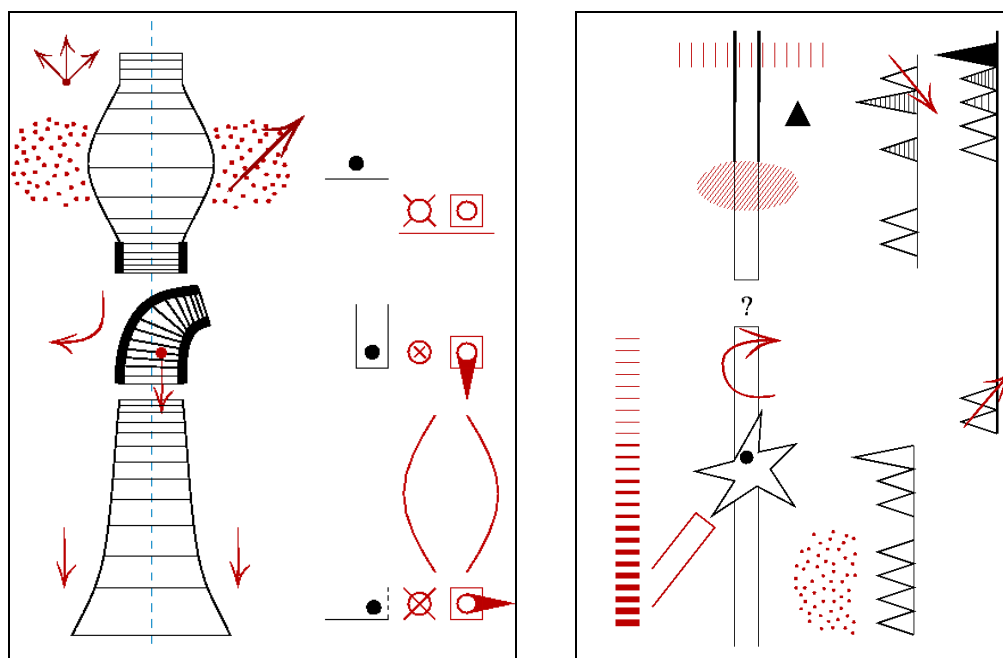


Figure 6: On the left, the scheme shows a use of the space and motion notation for a road portion. On the right, the scheme shows the orientation notation for another road portion [Appleyard *et al.*, 1964].

On the road, a driver is orienting himself in the general environment. The orientation sense is certainly one of the most complex and conceptual aspect along the road. Appleyard, Lynch *et al.* define orientation sense as “the general image of the road and the landscape that develops in the mind, partly as a results of what is presently visible, partly as a result of the memory of past experience” [Appleyard *et al.*, 1964]. In order to generate diagrams which represent an orientation sequence, they complete the notation of Lynch from [Lynch, 1960] and add to it a specific notation for goal approach. The result is illustrated by the right side of the Figure 6. While the left side of the scheme shows the road image and its events, the right side is the goal approach diagram.

### 2.3.2. ‘Envirotecture’

In [Thiel, 1969], Thiel provided another notation of space, motion and orientation in urban environments. His notation was inspired by the *labanotation* [Hutchinson, 1954] which is used for choreography and describes the eye direction, movement speed and the body spatial position. Unlike the precedent notation, the notation of Thiel does not limit to the highway field. It extends itself to most general fields, which include urban planning and architecture, that Thiel groups under the term of *envirotecture*. The specificity of this method is to use a hemispherical projection where the vision axis is considered as a symmetrical axis for a hemisphere of 180° which includes a half part of the visual world. For Thiel the visual world is divided into three-dimensional objects, two-dimensional surfaces, screens which are intermediate elements between objects and surfaces, and relations between these elements also called SEEs (Space Establishing Elements).

### 2.3.3. Conclusion

An abstract notation to represent visual events allows to describe quickly and intuitively intentions in urban or architectural projects. However, a single abstract scheme could have several interpretations. For example, with the notation of Appleyard *et al.*, the same symbol represents a river, a chain of mountains, or large wall. Hence, this notation should be completed by another type of document schemes of visual field or a text.

## 2.4. Regions of homogeneous aspect

The division of space into regions, where visual informations are homogeneous, allows to represent visual events which appear as transitions between two regions. We will present different kinds of methods which compute partition of two-dimensional or three-dimensional spaces.

### 2.4.1. Two-dimensional methods

The visual field is exposed to two kinds of change [Georgia Tech Research Corporation, 2001][Peponis *et al.*, 1997]. The first can be called *continuous change* and relates to our changing perspective views of the surfaces or partially visible surfaces. The second can be called *discrete change* and is associated with the appearance of clearly identifiable and finite elements of shape, namely discontinuities as defined below. Provided by Peponis *et al.*, the *e-partition* describes a structure of the changing visual field from the viewpoint of discrete changes in visual information.

In this section, what we call an environment is a wall configuration in a two-dimensional plan. A wall is a real surface in Benedikt's terms [Benedikt, 1979], that is to say an opaque, material, visible surface (we disqualify the sky, glass, mirrors, mist, and perfectly black surfaces). These walls provide discontinuities like edges of freestanding walls and the corners formed at the intersection of two wall surfaces [Peponis *et al.*, 1997]. The walls are represented as lines without thickness.

**Convex partitioning.** A space is said convex when any two of its points can be joined by a segment that lies entirely within the space. According to Hillier and Hanson, the convex spaces correspond to our intuition of two-dimensional spatial units which are completely available to our direct experience from any of their points. A first method uses circles in order to determine the convex partition [Hillier and Hanson, 1984]. A second one consists in extending wall surfaces, like with s-partition method (see below), and producing the largest overlapping convex spaces [Hillier, 1996]. A last method consists in partitioning the environment in order to provide the simplest representation of its spatial structure [Peponis *et al.*, 1997]. This method is known as the *m-partition* or *minimal-partition* because it produces the minimal number of the largest convex spaces which does not overlap. One of the drawbacks is that none of these methods take care of the visual events provided by an environment.

**s-partition.** The e-partition is an extend of another method proposed by Hillier, called *surface-partition* or *s-partition* [Hillier, 1996]. The s-partition consists in extending walls inside the plan, on the same way as the scheme in Figure 7. Hence, we have an environment divided by *s-lines* into *s-spaces*. Each time an observer crosses an s-line, an entire surface either appears into the visual field or disappears outside it. Thus transitions from one s-space to another are associated with changes in the available visual information about shape. However, the reverse is not true. Surfaces and parts of surfaces may appear or disappear without crossing an s-line [Peponis *et al.*, 1997].

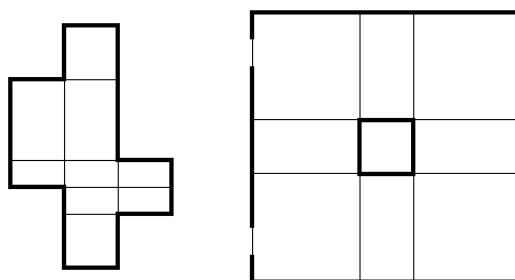


Figure 7: s-partitions of two plans.

**e-partition.** The e-partition, or *end-point partition*, method does not extend only the walls but also diagonals. A *diagonal* is defined as a line that joins two discontinuities without crossing a wall, and some of them can be extended without going outside of the shape. Figure 8 shows examples of e-partitioning obtained by extending both walls and diagonals.

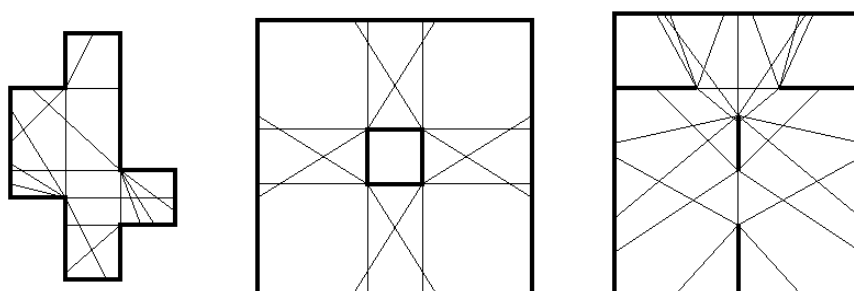


Figure 8: e-partitions of three plans.

With this method, we obtain a new convex partition which has two singular properties: “first, every time we cross a demarcation line, a discontinuity either appears into or disappears from our field of vision. Second, the convex subshape defined by this partition are informationally stable” [Peponis *et al.*, 1997]. On the other hand, the e-partition can be used to calculate the *integration* of environment subspaces. The integration is defined in [Hillier and Hanson, 1984] as the way in which the parts of a system are linked into a whole. A space is said more integrated when all other spaces can be reached after traversing a small number of intervening spaces, and it is less integrated when the necessary number of intermediate spaces increases. Figure 9 shows the result of integration computation for an entire environment *e-partitioned*.

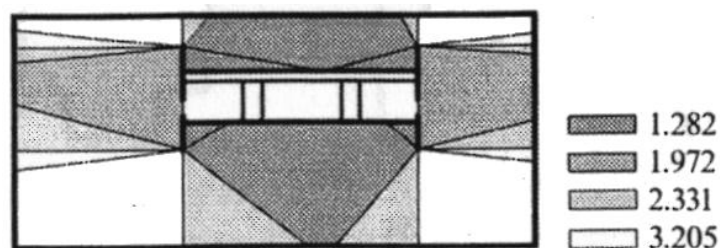


Figure 9: The integration pattern of Farnsworth House [Peponis *et al.*, 1997].

#### 2.4.2. Three-dimensional methods

**Aspect graph.** The 3D space can be divided into visually homogeneous regions. We say that a region is visually homogeneous if the topological structure of the scene image is the same for all the viewpoints in this region. This space subdivision is called *VSP* (Viewpoint Space Partition) [Plantinga and Dyer, 1990][Durand, 2000]. It can be generated by using a perspective or an orthographic projection (see Figure 10). The VSP allows to define a dual structure called *aspect graph*. An aspect graph records the topological structure of the

visibility in each region. Each vertex represents a visually homogeneous region, and two vertices are connected by an edge whenever their viewpoint regions are themselves adjacent.

The boundaries between two adjacent aspects are determined by analysing the *visual events*. These visual events are transition regions where the image aspect is changed (i.e. a vertex or an edge of a polygon appears or disappears). Plantinga and Dyer define different kinds of visual events:

- *vertex-vertex*: for a given viewpoint, the vertex of a polygon is in front of a vertex from another non-coplanar polygon;
- *vertex-edge*: for a given viewpoint, the edge of a polygon is in front of a vertex from another non-coplanar polygon;
- *edge-edge*: for a given viewpoint, the edge of a polygon intersects on the projection of an edge from another non-coplanar polygon;
- *edge-edge-edge*: for a given viewpoint, three edges from different non-coplanar polygons intersect into a point on the projection.

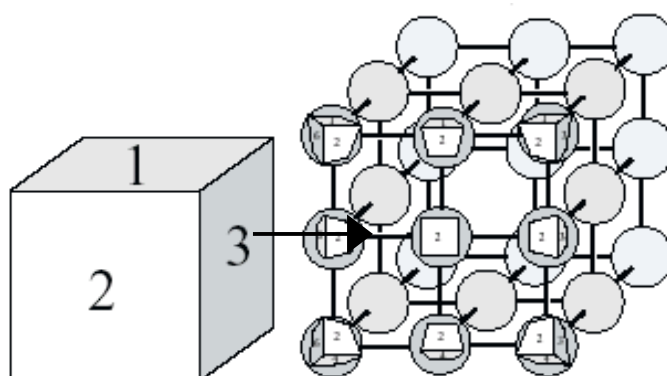


Figure 10: Aspect graph of a cube in perspective projection [Durand, 2000].

The aspect graphs and the study of visual events allow to compute the exact meshing of a scene, or discontinuity meshing [Hedley, 1998], in order to have a more realistic render of shading zone. One limitation of the aspect graphs method is that it only considers polyhedrons. Nevertheless, the method has been extended to compute aspect graphs of smooth and piecewise smooth objects [Petitjean, 1996]. Nowadays, the generation of visibility graph for curved objects is a research topic.

**Visibility skeleton.** The *visibility skeleton* is a data structure that records visual properties and visual relationships between objects in a three-dimensional scene [Durand *et al.*, 1997]. It provides a global knowledge of the scene. In a lot of algorithms relating to aspect graph computations, and to antipenumbra or discontinuity meshing, visibility changes are characterized by relations between vertices and edges.

Durand *et al.* consider two basic relations. The *extremal stabbing lines* are lines incident to four edges. Thus, an extremal stabbing line can be a vertex-vertex line, a vertex-edge-edge line, a quadruple edge line, etc. (we consider a vertex as the intersection of two edges). Extremal stabbing lines can be associated to faces of polyhedral objects. As a result, this kind of lines have zero degree of freedom. On the other hand, Durand *et al.* define the *line swaths*. A swath is a surface swept by extremal stabbing lines when they moved after relaxing exactly one of the four edges defining the line. This particular lines are line swath. It has one degree of freedom. To put it more precisely, a visibility skeleton is a graph where vertices represent extremal stabbing lines and edges are line swaths.

On the left side of Figure 11, An extremal stabbing line (VE1E2) is defined by two swaths (VE1 and VE2). These two swaths are fixed on the vertex V, VE1 moves on the edge E1, and VE2 on the edge E2. Another swath appears on the left side of the scene (VE1')

which divides the polygon which contains E2. The right side of Figure 11 represents the visibility skeleton of the scene: each extremal stabbing line is a vertex and each adjacent swath is an adjacent edge.

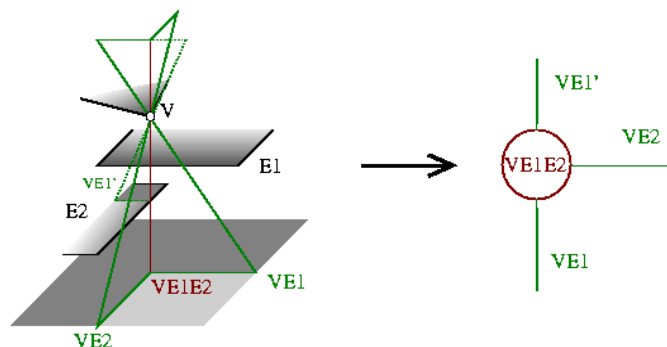


Figure 11: Visibility skeleton construction.

#### 2.4.3. About space partitioning

There are some drawbacks to partition space into homogeneous regions. For e-partition method, Teller notices that the data amount, the computation time, and the pertinence depend tightly on the definition level required for the model [Teller, 2001]. Hence, discontinuity apparition, frequent in urban scenes, contributes to complicate the e-partition representation. What is more, the method is not appropriated for environments which contain curves.

On the other hand, the aspect graph is not really used in computer graphics because of “the difficulty of robust implementation of exact methods, huge size of data-structure and the lack of obvious and efficient indexing scheme” [Durand, 2000]<sup>3</sup>.

Some of these remarks are also valid for the visibility skeletons. So, we could ask about the quality of these methods in a view to represent visual events inside a large model of a city, for instance. However, they allow, more locally, to do good study of some environments or objects.

### 2.5. Conclusion

There are questions about the realism of a representation. Some methods consider what we really see and others what we expect to see. But the pertinence of a representation involves problems of time and of space in order to generate it. Nevertheless, the methods we survey provide a set of techniques which can be highlighted, like spherical projection or space partitioning. From another viewpoint, some of them provide good methods for local study of the visual perception with a good definition level. However, all of these methods are not sufficient to achieve analysis.

## 3. Space characterization

A representation is a passive way to provide a new interpretation for a set of objects. An active way is to provide also a set of measures to characterize this set, allowing to deduce the sensations produced.

The purpose of this section is to survey some methods which allow to deduce the sensations produce by a space and more specifically by an urban environment.

### 3.1. Isovist

To analyse the visible space, Benedikt introduced in 1979 the isovists. First used for landscape analysis, Tandy introduced *isovist* term in [Tandy, 1967], and presented it as a

<sup>3</sup> A good discussion of the pros and the cons is given in [Faugeras *et al.*, 1992].

method of “taking away from the [architectural or landscape] site a permanent record of what would otherwise be dependent on either memory or upon an unwieldy number of annotated photographs.” By using this approach and including the Gibson’s perception theory [Gibson, 1966, 1979], Benedikt proposed a set of analytic measures on isovist properties to be applied to achieve quantitative descriptions of spatial environments. Then, he provides another definition of isovist:

“An *isovist* is the set of all points visible from a given vantage point in space and with respect to an environment.” [Benedikt, 1979]

To have a more formal notation, let  $P$  be an environment with a configuration of walls<sup>4</sup> and  $x$  a vantage point in  $P$ . An isovist  $V_{x,P}$  (or  $V_x$  if  $P$  is understood) generate from  $x$  is the set of all points in  $P$  such as:

$$V_{x,P} = \{y \in P \mid xy \cap P = xy\}$$

That is,  $V_{x,P}$  consists of all points  $y$  in  $P$  with the property that  $y$  is visible from  $x$ .

Figure 12 presents two isovists (in grey on the schemes) generated in a same environment from distinct vantage points, which are represented by small squares. On the one hand, we can notice that isovists (their shapes and their dimensions) entirely depend on their vantage point location. On the other hand, isovists are polygons and their boundaries can be divided into two parts: boundaries common with a wall or a part of a wall, and boundaries which cross  $P$ , called *occluded boundaries* of  $V_x$ .

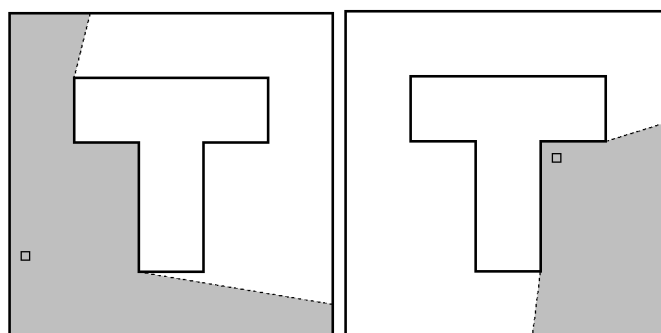


**Figure 12: Two 2D isovist polygons generated in the same environment from distinct vantage points.**

To have a comparison, isovist is a method to structure space that could be compared to the ambient optic array proposed by Gibson [Gibson, 1966, 1979]. Gibson defined an optic array as a set of nested solid angles corresponding to surface elements in the environment. Moreover, Benedikt states that “the isovist is simply this optic array, with wavelength and intensity information omitted” [Benedikt and Burnham, 1985].

### 3.1.1. Diagram drawing

Benedikt and Davis propose an algorithm to compute isovists by using a triangulation of the isovist polygon around the vantage point [Davis and Benedikt, 1979]. Here, we show other methods to compute isovists.

One of them calculates the radial distances for a given subset of vision angles, between 0 and 360° [Wise, 1985]. This method allows to considered curved wall and to directly draw graphs of radial distances (Figure 13). The centre of this graph represents the direction left to right from the vantage point. Moving to right on the graph means moving in the counter clockwise direction around the vantage point. We can notice some singularities in the graph like peaks, troughs or vertical breaks. These singularities correspond respectively to

<sup>4</sup> We call a wall, an opaque, material, visible surface, humanly perceivable [Benedikt, 1979].

appearance of convex corner, concave corner and region hidden from the visual field. Figure 14 shows some correspondences between the discontinuities of the environment and the graph.

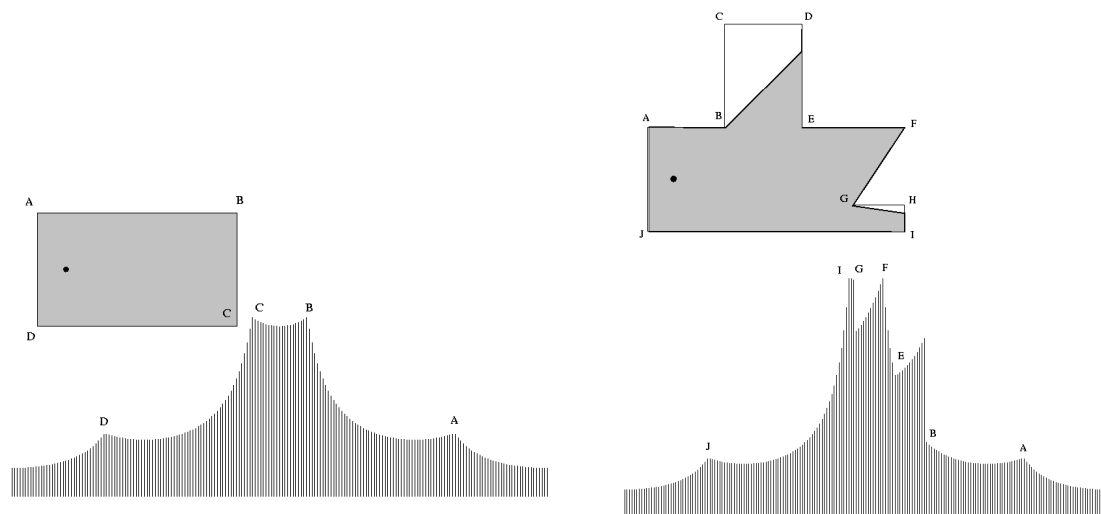


Figure 13: Two 2D isovist diagrams generated in two environments.

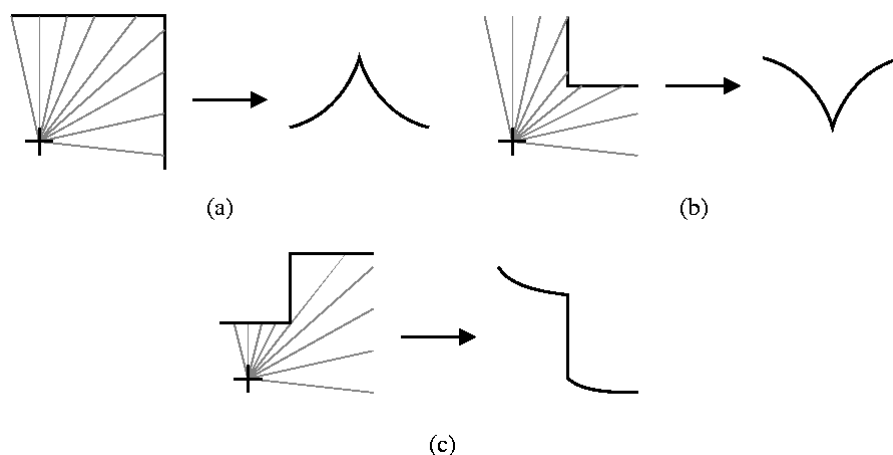


Figure 14: Examples of isovist behaviour. A convex angle is represented by a peak on the graph (a) and concave angle by a trough (b). If a part of the environment is unseen from the vantage point, it generates a vertical break in the graph (c).

Another way to represent isovists is to draw an isovist sequence, computed along a route, on a surface (Figure 15). This kind of representation shows the evolution of environment discontinuities along the route.

However, this kind of representation is not an easy way to interpret isovists and to deduce characteristic from an environment. Nevertheless, isovist can be considered as a polygon or as a distribution function. It allows to use geometrical and statistical measures.

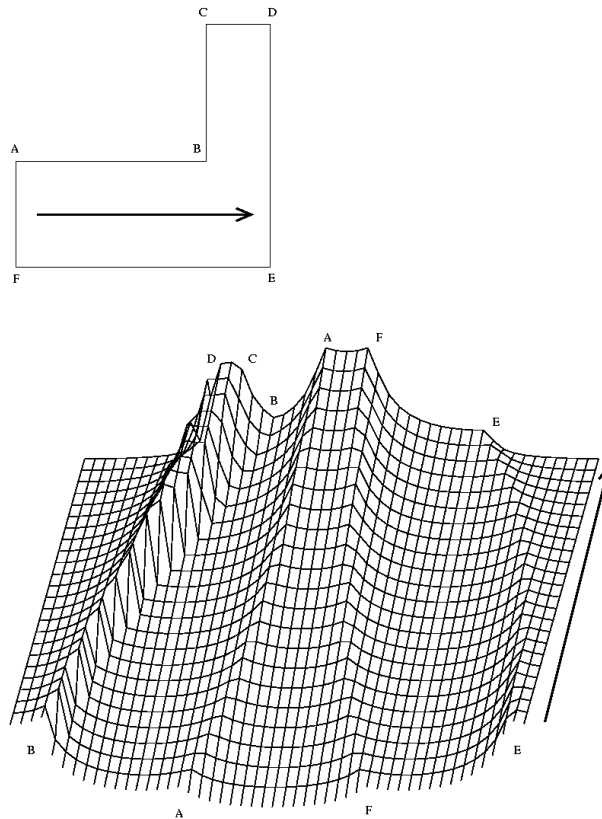


Figure 15: 3D diagram representation of an isovist sequence (following the arrow).

### 3.1.2. Isovist measures

In order to give an interpretation of each isovist, Benedikt identified different geometric measures [Benedikt, 1979][Davis and Benedikt, 1979].

**Area and perimeter.** The area and the perimeter measure how much space can be seen from a vantage point and how much environmental surface can be seen from this point [Benedikt, 1979]. In order to obtain the area of an isovist, we can consider isovist as a continuous set of radial distances. Hence, an isovist is a polar function. According to [Weisstein, 2001] and [Batty, 2001], the area  $A_x$  of a given isovist  $x$  is:

$$A_x = \int_0^{2\pi} r_x^2(\theta) d\theta$$

Where  $r_x$  is a function that calculates the radial distance in the isovist  $x$  for a given angle  $\theta$ .

If we consider isovists as polygons determined by their vertices  $v_i$ , the perimeter  $B_x$  of an isovist is:

$$B_x = \sum_i \|v_i v_{i+1}\|$$

Where  $\|MN\|$  is the Euclidean distance between the two points  $M$  and  $N$ .

**Circularity.** From  $A_x$  and  $B_x$ , we can also calculate the circularity of an isovist. This measure compares a polygon to a circle from a formal viewpoint. For a circle with the area  $a$  and the perimeter  $p$ , we have the relation  $p^2 = 4\pi a$ , then its circularity  $\Psi = 4\pi a/p^2$  is 1. For any other geometrical figure, this ration is less than 1; but if  $\Psi$  is near from 1 the polygon is similar to a circle, and if  $\Psi$  is near from 0 the polygon is similar to a straight line.

The circularity  $\Psi_x$  for an isovist  $x$  is thus the ratio:

$$\Psi_x = \frac{4\pi A_x}{B_x^2}$$

In his papers, Benedikt uses two other forms to calculate the circularity [Benedikt, 1979][Davis and Benedikt, 1979]. The first one is given by an inversion  $N_x = 1/\Psi_x = B_x^2/(4\pi A_x)$ ; the second one is called compactness and is given by  $B_x^2/A_x$ . For Batty [Batty, 2001], the compactness can be calculated by the ratio between the mean radial length and the maximal radial length for an isovist, or by the ratio  $\sqrt{(A_x/\pi)}/(B_x/2\pi) = \sqrt{\Psi_x}$ . Finally, Conroy [Conroy, 2001] provides another circularity equation where the perimeter is replaced by mean radial distance of the isovist:  $\Psi_x = (\pi|\bar{r}_x|^2)/A_x$ . The circularity formula used here is equivalent to the circularity formula used by Teller for open spaces computation [Teller, 2001] (see section 3.3).

**Variance and skewness.** Benedikt proposes two other measures. The first one is called the variance and calculates the dispersion of the perimeter relative to the vantage point  $x$ . The second one is the skewness and calculates the asymmetry of the dispersion of the perimeter to  $x$ .

In order to calculate these two measures, Benedikt uses the second and the third radial moment  $M_{2,x}$  and  $M_{3,x}$ . The  $p$ -th centred radial moment  $M_{p,x}$  for an isovist  $x$  is given by:

$$M_{p,x} = \frac{1}{2\pi} \int r_x(\theta) \cdot (\theta - \bar{r}_x)^p d\theta$$

Where  $\bar{r}_x = \int r_x(\theta) \cdot \theta d\theta$  is the mean value of function  $r_x$ . The second radial moment allows to calculate the standard deviation coefficient which is given by  $\sigma_x = \sqrt{M_{2,x}}$  and could be compared to the equivalent method of Teller (see section 3.3).

**Drift.** Another measure is provided by Conroy, called *drift*, which calculates distance between the location from which the isovist is generated and its centre of gravity [Conroy, 2001]. Drift tends to be minimal at the centre of spaces and along centre-line of roads.

### 3.1.3. Applications of isovists

Isovists can be helpful to solve some problems where the visibility is a predominating factor. One of them consists to preserve the privacy. The problem is to find “[...] an optimum balance [...] between the ‘information’ which comes to a person and that which he puts out” [Canter and Kenny, 1975]. Isovist size measures, such as  $A_x$  and  $B_x$ , approximate the amount of this kind of information [Benedikt, 1979]. Other problems consist in seeing much without being overly exposed or reduce the security by minimizing the occlusivity fields (spaces leaved unseen from a point), for example. This kind of problems can be treated using isovist theory.

In his report [Wise, 1985], Wise used isovist in order to improve the design of spatial cabins. For him, there are three main concepts: the visual aspects, the kinaesthetic aspects and the social logic (with the same meaning as [Hillier and Hanson, 1984]). For the visual aspect, Wise was interested in the perceived size of an environment, its apparent orientation and its affective connotation. The isovist analysis allowed him to have a direct method to measure visual qualities.

Finally, an isovist variation, called *viewshed*, is used in landscape analysis [Burrough, 1986][Fisher, 1995]. The originality of this method is that it takes into account the level informations of all portion of the ground. Hence, the viewscheds allow to locate the hidden dips from a viewpoint and also the ground area visible from this point.

### 3.2. Visibility graphs from Space Syntax

Instead of representing the visibility area as isovist do, Turner *et al.* provides a data structure, called *visibility graph*, representing the intervisibility relationships between points of an environment [Turner and Penn, 1999][Turner *et al.*, 2001][Turner, 2001].

The visibility graphs are topological graphs where each vertex is associated to a vantage point on a map. The presence of an edge between two vertices involves that one “can see” and “can be seen from” the other. Each vertex is disposed regularly on a virtual grid. In mathematical terms, let  $G = (V, E)$  be a visibility graph, where  $V = \{v_1, v_2, \dots, v_n\}$  is a set of vertices and  $E \subseteq \{e_{ij} \mid i, j \in 1, \dots, n\}$  a set of edges. Each vertex  $v_i$  is associated to a location  $(x, y)$  on a map, and we denote the edge joining  $v_i$  and  $v_j$  as  $e_{ij}$ . In a visibility graph, there is an edge  $e_{ij}$  if and only if  $v_i$  can see  $v_j$  and  $v_j$  can see  $v_i$  (this involves  $e_{ij}, e_{ji} \in E$ ).

Figure 16 shows the beginning of a visibility graph construction. We can notice that the white vertex neighbourhood is included in the isovist generated by these vertices (in grey on the scheme). When the visibility graph construction is completed, this property allows us to measure visibility informations on each vertex without generating corresponding isovist.

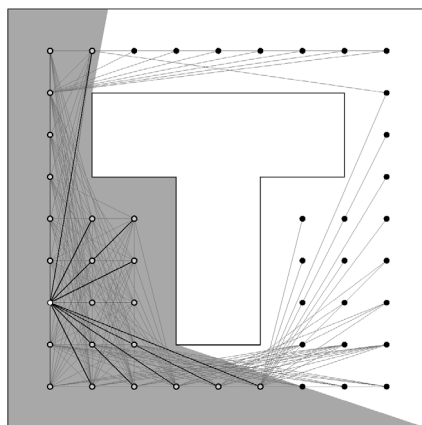


Figure 16: A step in the visibility graph construction.

#### 3.2.1. Visibility graph measures

Like isovist analysis, the visibility graphs were mainly applied to house planning. However, in [Batty, 2001], Batty extended visibility graph applications to urban analysis.

In this paper, we will introduce the possible measures in urban scene by illustrating them with an actual case in Nantes. We present an analysis, with our implementation of visibility graph, of *place du Martray* and a part of *rue Sarrazin* in Nantes. This two urban locations are relatively enclosed locations and easy to model<sup>5</sup>. With a 12 906 vertices division on a 205 m × 265 m map, each vertex covers a surface of 1.4 m<sup>2</sup>. The Figure 17 shows the model and the studied part. Considering an outlying zone, enables to have more realistic measures for the studied zone.

<sup>5</sup> There is another reason why we choose these locations that we will explain later.

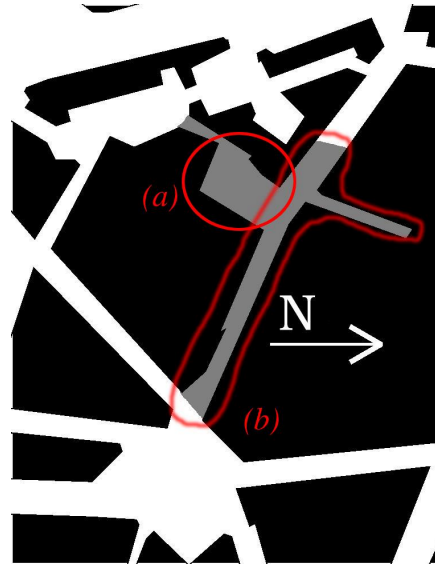


Figure 17: The study area corresponds approximately to the grey zone. It corresponds to the *place du Martray* (a) and a part of the *rue Sarrazin* (b) in Nantes.

**Neighbourhood size.** One of the first measure proposed by Turner et al. is the neighbourhood size  $|N_i|$  which calculates the adjacent vertices number for each vertex. As each vertex covers small map surface, the neighbourhood size of vertex  $v_i$  is proportional to the isovist area  $A_i$  for the vantage point it represents.

$$A_i \approx \delta \cdot |N_i| = \delta \cdot \left| \{v_j \mid e_{ij} \in E\} \right|$$

Where  $\delta$  is a coefficient corresponding to the part of surface covered by each vertex. On the upper left of Figure 18, we represent the neighbourhood size for each vertex on the map. The darker is a point, the larger is its visibility area.

**Clustering coefficient.** Another measure, provided by Turner *et al.*, is the clustering coefficient  $\gamma_i$ . It compares the number of adjacent edges in the neighbourhood of a vertex with its theoretical maximum:

$$\gamma_i = \frac{\left| \{e_{jk} \in E \mid v_j, v_k \in N_i\} \right|}{|N_i| \cdot (|N_i| - 1)}$$

The clustering coefficient gives a measure of the apparent space convexity from a location. If  $\gamma_i$  is near from 1, the most part of the vertices in the neighbourhood are visible between them. This implies that the generated isovist would be convex. If  $\gamma_i$  is near from 0, then the space looks like a star. Another way to interpret  $\gamma_i$  is about the visibility information preservation. By moving inside a region where  $\gamma_i$  is near from 1, the changes of information would be less important than moving inside a region where the  $\gamma_i$  is near from 0.

**Mean shortest path length.** The shortest path between two vertices  $v_i$  and  $v_j$  in a graph is the least number of edges  $d_{ij}$  between them. The mean shortest path length  $\bar{L}_i$  for a vertex  $v_i$  is simply the average of the shortest path lengths from that vertex to every other vertices in the graph.

$$\bar{L}_i = \frac{\sum_{v_j \in V} d_{ij}}{|V|}$$

The mean shortest path length provides a measure about visual accessibility of a location with respect to observer movement. That is to say it allows to estimate the average number of movements necessary before a location can be seen. As it is a global measure, it depends on the model size.

**Visual distances.** In [Batty, 2001], Batty provides measures about the distance between one vertex and vertices in its neighbourhood. He defines the maximum distance  $d_i^{\max}$  that can be seen from the vertex  $v_i$ , the minimum distance  $d_i^{\min}$  and the average distance  $\bar{d}_i$ :

$$d_i^{\max} = \max_{v_j \in N_i} \{ \|v_i v_j\| \} \quad d_i^{\min} = \min_{v_j \in N_i} \{ \|v_i v_j\| \} \quad \bar{d}_i = \frac{\sum_{v_j \in V} \|v_i v_j\|}{|N_i|}$$

Where  $\|v_i v_j\|$  is the Euclidean distance between locations represented by  $v_i$  and  $v_j$ .

To these measures we can add the distance standard deviation  $\sigma_i$  for each vertex. As it indicates the range of radial distances for any single isovist, the standard deviation gives us an idea of the environment shape regularity.

$$\sigma_i = \sqrt{\frac{\sum_{v_j \in V} (\|v_i v_j\| - \bar{d}_i)^2}{|V|}}$$

**Other measures.** In [Turner, 2001], Turner proposes other measures for analysing visibility graphs. The first one is taken from the theory of Hillier and Hanson [Hillier and Hanson, 1984] and allows to calculate a control value  $c_i$  for a location. According to [Hillier and Hanson, 1984], the control gives a local measure which value varies around 1. If the value for a location is above 1 then the control is strong, however the control is considered as weak.

$$c_i = \sum_{v_j \in N_i} \frac{1}{|N_j|}$$

Another measure gives an idea of the frequency distribution of the shortest path length (or depth). This measure  $s_i$  is called point depth entropy and is calculated using the Shannon's formula.

$$s_i = \sum_{d=1}^{d_{\max}} -p_d \log p_d$$

Where  $d_{\max}$  is the maximum length from the current vertex and  $p_d$  is the frequency of the length  $d$  from the current vertex. According to Turner, the "point depth entropy can give an insight into how ordered the system is from a location" [Turner, 2001].

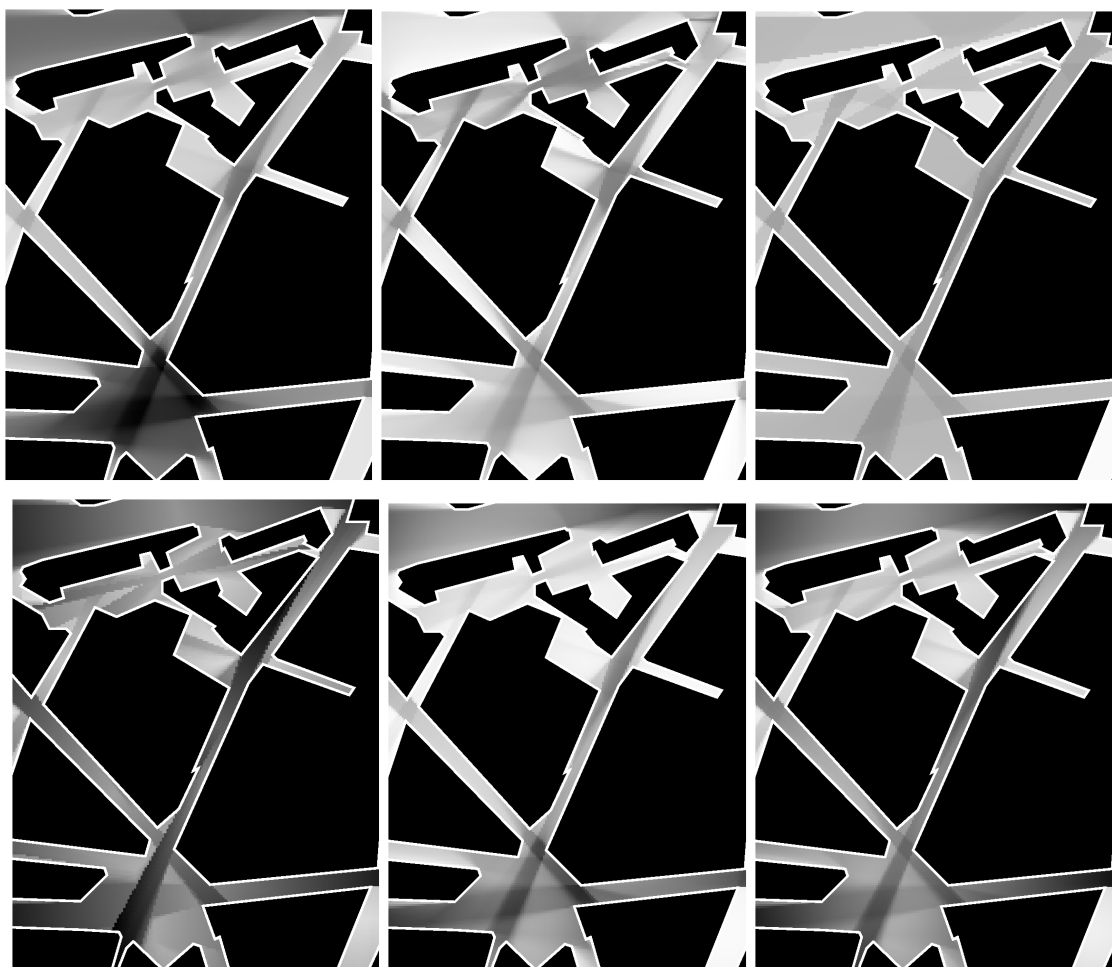


Figure 18: Six measures on a 12 906 vertices graph (from upper left to lower right): visibility area, clustering coefficient, integration ratio, maximum distance, average distance, distance standard deviation.

### 3.2.2. Comments on results

At first sight, it is not easy to distinguish the six pictures in Figure 18. For *Place du Martray*, a division appears with the clustering coefficient, the maximum distance, and the distance standard deviation due to dead end in the north of *Rue Sarrazin*. With the other measures, the brightness from all locations of the place is relatively the same and seems to delimit it. For *Rue Sarrazin*, the measures have interesting value in the east end, and near *Place du Martray*. Inside the street, they do not seem to vary a lot. Near *Place du Martray* and in the east side of the street, the space shape is not convex and provides more visibility area; this implies a local darkening of the coefficients.

Actually, the cathedral appears in the visual field when we walk in the east side of *rue Sarrazin*. It is *cathédrale Saint-Pierre* located 700 m far from the studied area. It is not shown in figure 16 and would not be correctly studied by the visibility graph even if it were drawn on the map. This is done because of walls which stand between the viewpoint and the cathedral. But as they are in a dip, they are taken into account by two-dimensional methods<sup>6</sup>, though they do not appear in the visual field. This particularity shows a mistake linked to the map transformation of the urban environment.

### 3.2.3. Visibility graph criticism

With *visibility graph*, Turner et al. provide a regular data structure that helps to analyse

<sup>6</sup> The same problem appears with the isovist method.

visibility in 2D environments [Turner and Penn, 1999][Turner *et al.*, 2001][Turner, 2001]<sup>7</sup>. Its main advantage is to structure environment and to record visibility informations which is considered as a first-order relation. In fact, visibility graph analysis can be considered as an extend or an alternative to isovist field analysis (see section 3.1).

However, we can highlight two weaknesses for the visibility graph method. Above, we have seen the results of this method could be altered by the two-dimensional transformation of the urban environment. In an other viewpoint, the computation time of the visibility graph increases rapidly with its resolution. For example, let's suppose an empty square environment which is 5 km length for each edge. For a definition of 1 m<sup>2</sup> per vantage point, it is necessary to generate one million points, producing a matrix of  $6.25 \times 10^{14}$  elements for the graph representation. As some algorithms are  $O(n^2)$  in the worst case (like the algorithm for graph construction or the measure for the mean shortest path length)<sup>8</sup>, the processing time would theoretically be around one billion ( $10^{12}$ ) years with an 1 GHz computer. But, a solution to solve this problem would perhaps be to optimise these algorithms.

Thus, the visibility graph method seems to be adapted to analyse parts of a plane city, or larger models with a lower but sufficient resolution.

### 3.3. Open space indicators

Unlike isovist or visibility graph analysis methods, Dupagne and Teller consider the third dimension and analyse the urban scene through the spherical projection. Dupagne and Teller reuse the “urban boxes” concept from Camillo Sitte, and analyse shapes formed by buildings [Dupagne *et al.*, 1997][Teller and Azar, 2001][Teller, 2001].

#### 3.3.1. Sky opening

Sky opening is defined as the ratio between the sky area in isoaire projection and the area of the circle in which image is projected. This coefficient is relative to the enclosure sensation in a scene: it is valuated to 0 in a closed volume and to 1 on a plane without any object.

In a urban scene, the sky opening coefficient changes with the observer location. Near a wall, the scene seems to be more closed than in the middle of a street or of a place. It is possible then to draw the sky opening coefficient variation on a map. Figure 19 shows the sky opening coefficient variation map for *la Grand'Place d'Arras* [Teller, 2001]. We can notice the coefficient values in the streets, near the wall in places and in the middle of places.



Figure 19: Sky opening map for *la Grand'Place d'Arras* [Teller, 2001].

<sup>7</sup> The visibility graph analysis functions are implemented in a software called Depthmap, available at <http://www.vr.ucl.ac.uk/depthmap>.

<sup>8</sup> A  $O(n^2)$  algorithm has a computation time proportional to the square number of data.

### 3.3.2. View depth

One of the drawbacks of sky opening measure (with spherical projection) is to let the same visual weight for a high and far volume than for a smaller but closer volume. To correct or to complete the sky opening coefficient, Teller analyses the view distances with two methods [Teller, 2001].

The first one calculates mean view length  $L_m$ , for a given vantage point, of distances  $l_i$  between the vantage point and visible faces  $f_i$  weighted by their area  $s_i$  in isoaire projection:

$$L_m = \frac{\sum_i s_i l_i}{\sum_i s_i}$$

This measure is independent from the sky opening. Thus, a mean length of faces 50 m far from the observer which occlude 80 % of sky surface is equivalent to a face configuration which occludes 20 % of sky surface with the same distance from the observer. In order to differentiate this two cases, Teller proposes to take into account the occluded sky surface:

$$L_c = \frac{\sum_i L_i \cdot S_i}{\sum_i S_i}$$

$S_r$  is the visible sky surface and the result  $L_c$  is called the typical length. This measure varies between the mean length and the infinity depending on whether the faces covers 100 % or 0 % of the sky surface.

### 3.3.3. Sky regularity

The statistical tools can provide different kinds of indicators relative to the sky shape and its regularity. To realize these measures, Teller proposes to use the equidistant spherical projection which allows to hold the visible height proportions with respect to a vantage point. Thus, we can calculate the maximal and the minimal height, the mean height or the height standard variance. We can add the sky surface compacity  $C = 4\pi A/P^2$ , as we saw above in the isovist section (section 3.1).

All the results obtained by these measures could be compared to those obtained by isovist analysis. Actually, it would be interesting to compare 3D analysis methods with 2D ones for similar measures.

### 3.3.4. Spreading and eccentricity

A measure like compacity is extremely sensitive to noise. The increase of the object definition causes apparitions of peaks which increase the perimeter without modifying the area a lot. In this case, the change generates an important modification in the compacity value. To have a less sensitive measure, Teller proposes to use the moment of inertia of sky shape. The  $(i + j)$ -th moment of inertia  $M_{ij}$  of an homogeneous shape is computed by the formula:

$$M_{ij} = \iint x^i y^j dx dy$$

In this section, we focus on the second moment of inertia providing  $M_{20}$ ,  $M_{11}$  and  $M_{02}$  values which are sensitive to location and orientation. The reference axis orientation is given by the eigenvalues  $I_1$  and  $I_2$  of the matrix of inertia  $M_I$ :

$$M_I = \begin{pmatrix} M_{20} & M_{11} \\ M_{11} & M_{02} \end{pmatrix}$$

Thus,

$$I_1 = \frac{M_{20} + M_{02} - \sqrt{(M_{20} - M_{02})^2 + 4M_{11}}}{2}$$

$$I_2 = \frac{M_{20} + M_{02} + \sqrt{(M_{20} - M_{02})^2 + 4M_{11}}}{2}$$

The two last measures is used by Teller to calculate the spreading  $S$  and the eccentricity  $E$  of the space shape:

$$S = \frac{I_1 + I_2}{M_{00}^2}$$

$$E = \frac{I_1}{I_2}$$

Where  $M_{00}$  is the 0-th moment of inertia which corresponds to the area.

The spreading  $S$  calculates the mass dispersion of a figure and is similar to the compacity. Nevertheless, the spreading does not depend on the perimeter; thus it is less sensitive to the shape noise. The lower limit of  $S$  is  $\pi/2$ , which is the spreading of a circle. The eccentricity  $E$  is a ratio which gives an idea of the symmetry of a shape with respect to its gravity centre. If the shape is symmetrical,  $E$  is 1; if it is not,  $E$  is greater than 1.

### 3.4. Visual accessibility of an object

In the previous sections, we have seen methods to analyse visual field of an observer in an urban environment. The purpose of this section is to show methods to analyse an object as seen by a set of observers.

#### 3.4.1. Visual accessibility in an urban environment

To measure the visual accessibility of an object, Nivet uses the term of *intermittence* [Nivet, 1998][Nivet and Siret, 1998]. The intermittence is a relation which qualify the visibility between an observer and an object in a scene. In fact, Nivet proposes two measures of intermittence: the space intermittence and the object intermittence. Those two measures allow to represent the visual accessibility.

The space intermittence  $I_e$  measures the proportion of points in a space from which a given object is totally or partly visible.

$$I_e = \frac{A(\text{sub\_space})}{A(\text{total\_space})}$$

The object intermittence  $I_o(p)$  measures ratio between the visible surface of an object from the point  $p$  and its visible surface from the same point if it were alone in the scene.

$$I_o(p) = \frac{A(\text{visible\_area})}{A(\text{total\_area})} = 1 - \frac{A(\text{hide\_area})}{A(\text{total\_area})}$$

Nivet uses the couple  $(I_e, I_o)$  in a view to qualify the visual intentions in the architectural projects. For example, the intention (1,1) means “see completely” or “from all point of the considered space, see the whole of the object”, and the intention (0,0) means “see nothing” or “do not see anything of the object from all point of the considered space”.

Another proposition was made by Morin in order to study the visual accessibility of *la Tour de Bretagne* in Nantes [Morin, 1995]. This work consists in using *Solene* [Groleau, 2002], a software dedicated to sun lighting simulation in urban environment, to determine the surfaces of the object seen or leave unseen.

### 3.4.2. Object visibility and landscape protection

Koglin and Rheinert [Koglin and Rheinert, 1999] propose a method for generating an optimal solution in order to build overhead lines. Their method is based on cost criterion, on optical impact criterion, and on “approval ability” criterion. To solve the optical impact criterion of overhead lines, they use a method developed at Saarland University [Koglin and Zewe, 1995] that takes into account the virtual size of the pylon looked at and the colour difference between pylon and background.

In their paper [Koglin and Zewe, 1995, 1996], Koglin and Zewe provide different measures mainly based on method of Groß [Groß, 1991]. The psychophysical factors relate to the observer density or the observer attention. The physical factors are given below.

- The *solid angle*  $\Omega$  is a measure of the apparent size of an object. It is calculated as the ratio between the object visible surface and the square of the visual distance from the observer ( $\Omega = S/d^2$ ).
- The *colour difference*  $\Delta E$  between the object and the background. The difference is calculated as the geometric distance between the colour values using the CIE  $Yxy$  colour space (where  $Y$  is the luminance, and  $x$  and  $y$  the colour location in the chart). Moreover, colours in the landscape depend on the atmospheric attenuation.

As a basis, these factors help to draw up a method for calculating the visibility of an object. One of the first measure is called the *location-specific visibility*  $S''$ . It calculates the optical impact of an object at a particular observer location. We suppose that each observer occupies an area  $\Delta A$  of size  $1 \text{ m}^2$ .

$$S'' = \frac{1}{\Delta A} \int_{\Omega} \Delta E d\Omega$$

The *total visibility*  $S = \int_A S'' dA$  gives a measure of entire visual impression caused by an object in the landscape. On the other hand, the *efficiency of camouflage* calculates the location-specific visibility for the same object from the same observer point but in front of a clear sky and without any obstacle leads to the maximum location-specific visibility  $S''_{\max}$ .

$$\eta'' = \frac{S''_{\max} - S''}{S''_{\max}}$$

### 3.5. About methods for space characterization

The methods described here give an original approach to characterize space, and usually provide a set of measures which allow to draw different kinds of visual variation map for a given environment. However, some of these methods (e.g. isovist, visibility graph, and methods for landscape analysis) are not adapted to large urban environment. Others methods, like the Nivet's method, intend to take up any other applications.

## 4. Conclusion

The visual interpretation of an urban environment needs a way to model it, with the aim to highlight some visible elements (e.g. shape, colour, visual events, etc.), and to analyse it in order to provide a characterization of the environment. In this paper, we saw different kinds of methods that allow to interpret the visual events.

In the section 2, we have presented several representation methods of visual field and of visual events. They provide a set of concepts which can be highlighted. For example, the spherical projection gives a mean to represent the whole visual world; the notations provided by Thiel or Lynch *et al.* use an abstraction of the visual world to represent what we see; the convex partition methods structure the environment into visually homogeneous regions.

However, these methods do not allow to achieve analysis. In section 3, we have seen three complete methods — isovist, visibility graph and sky opening indicators — that allow to analyse the visual perception of architectural and urban scene by using tools that come from statistics, graph theory, physics, and social logic of space. Other methods attend to only considered the visual perception of one object in a scene. They qualify the quantity seen of this object or the contrast it produces with the background (in order to analyse the efficiency of the camouflage for this object).

Most of these methods fail to model or analyse entire cities with a high level of resolution. All of them are reasonably good if the model is reduced to a district or a neighbourhood. Nevertheless, the methods we saw are mainly based on human visual system, in order to have a more intuitive representation of urban environment and to analyse it as human do. However, these elements are often limited to shape perception. With the aim to analyse visual events, it would be interesting to take into account the motion perception. Most of these methods are able to study it by generating space variation maps. But, they do not integrate the motion perception. Thus, it is difficult to interpret what a person can observe actually.

Similar questions raise about other attributes analysed by human visual system and about the visual events during a motion. For example, attributes like colour (study by the method saw in the section 3.4.2), texture or lighting are directly analysed by human visual system but leaved unexploited.

## References

- D. APPELYARD, K. LYNCH, and J. R. MYER (1964). *The view from the road*. MIT Press.
- M. BATTY (2001). Exploring isovist fields: space and shape in architectural and urban morphology. *Environment and Planning B: Planning and Design*, 28(1):123–150.
- M. L. BENEDIKT (1979). To take hold of space: isovists and isovist fields. *Environment and Planning B*, 6:47–65, 1979.
- M. L. BENEDIKT and C. A. BURNHAM (1985). Perceiving architectural space: From optic arrays to isovists. *Persistence and change*, pages 103–114.
- P. BOSSELMANN (1998). *Representation of Places*. University of California Press, 1998.
- P. A. BURROUGH (1986). *Principles of Geographical Information Systems for Land Resources Assessment*. Clarendon Press, Oxford.
- D. CANTER and C. KENNY (1975). *The spatial environment*. International University Press, New York.
- R. CONROY (2001). *Spatial Navigation in Immersive Virtual Environments*. PhD thesis, University of London.
- G. CULLEN (1961). *The Concise Townscape*. Butterworth Architecture.
- L. S. DAVIS and M. L. BENEDIKT (1979). Computational models of space: Isovists and isovist fields. *Computer Graphic and Image Processing*, 11(1):49–72.
- I. DE WOLFE (1963). *The Italian Townscape*. Architectural Press, Londres.
- A. DUPAGNE, M. JADIN, and J. TELLER (1997). *L'espace public de la modernité*. Études et Documents. Ministère de la région wallonne, direction générale de l'aménagement du territoire, du logement et du patrimoine, division de l'aménagement et de l'urbanisme.
- F. DURAND (2000). A multidisciplinary survey of visibility. In *Proceedings of*

SIGGRAPH'2000. [CD-ROM] Course notes CD-ROM, course #04: *Visibility: Problems, Techniques, and Applications*.

F. DURAND, G. DRETTAKIS, and C. PUECH (1997). The visibility skeleton: A powerful and efficient multi-purpose global visibility tool. In *Proceedings of SIGGRAPH'97*, pages 89–100, Los Angeles, California.

O. FAUGERAS, J. MUNDY, N. AHUJA, C. DYER, A. PENTLAND, R. JAIN, and K. IKEUCHI (1992). Why aspect graphs are not (yet) practical for computer vision. *Computer Vision and Image Understanding: CVIU*, 55(2):322–335.

P. F. FISHER (1995). An exploration of probable viewsheds in landscape planning. *Environment and Planning B: Planning and Design*, 22:527–546.

Georgia Tech Research Corporation (2001). Spatialist. [On-line] URL: <http://murmur.arch.gatech.edu/~spatial>.

J. J. GIBSON (1950). *The Perception of the Visual World*. The Riverside Press, Cambridge, Massachusetts, 1950.

J. J. GIBSON (1966). *The Senses Considered as Perceptual Systems*. Houghton Mifflin, Boston, MA.

J. J. GIBSON (1979). *The Ecological Approach to Visual Perception*. Houghton Mifflin, Boston, MA.

D. GROLEAU (2002). *Solene* : un outil de simulation des éclairagements solaires et lumineux dans les projets architecturaux et urbains. To be published in *Actes de l'École Thématique : La modélisation de la ville 2*, Nantes, 1999.

M. GROB (1991). The analysis of visibility — environmental interactions between computer graphics, physics, and physiology. *Computers & Graphics*, 15(3):407–415.

D. HEDLEY (1998). *Discontinuity Meshing for Complex Environments*. PhD thesis, Department of Computer Science, University of Bristol, August.

B. HILLIER (1996). *Space is the Machine*. Cambridge University Press.

B. HILLIER and J. HANSON (1984). *The social logic of space*. Cambridge University Press.

A. HUTCHINSON (1954). *Labanotation*. New Directions.

H.-J. KOGLIN and RHEINERT (1999). Multiobjective optimization with evolutionary algorithms for the synthesis of optimal overhead lines. In *Proceedings of ISAP 1999*, Rio de Janeiro.

H.-J. KOGLIN and R. ZEWE (1995). A valuation system for the visibility of overhead lines. *Engineering Intelligent Systems*, 3(4):195–203.

H.-J. KOGLIN and R. ZEWE (1996). Visibility as a criterion for the approval in the regional planning procedure. In *Proceedings of 12th Power Systems Computation Conference*, Dresden.

K. LYNCH (1960). *The image of the city*. MIT Press.

M. MORIN (1995). Lecture de la Tour de Bretagne – développement d'un outil de lecture de la ville (simulation de l'accessibilité visuelle). TPFE, École d'Architecture de Nantes.

M.-L. NIVET (1998). *De Visu : un logiciel pour la prise en compte de l'accessibilité visuelle dans le projet architectural, urbain ou paysager*. PhD thesis, Université de Nantes.

M.-L. NIVET and D. SIRET (1998). Simulation inverse de l'accessibilité visuelle en mileu

urbain. *Revue Internationale de CFAO*, 13(1):93–110.

P. PANERAI (1970). *Paysage urbain et analyse pittoresque*. Archives d'Architecture Moderne, Bruxelles.

P. PANERAI, J.-C. DEPAULE, and M. DEMORGON (1997). *Formes urbaines, de l'îlot à la barre*. Éditions Parenthèses, Marseille.

P. PANERAI, J.-C. DEPAULE, and M. DEMORGON (1999). *Analyse Urbaine*. Collection eupalinos. Éditions Parenthèses.

E. PANOFSKY (1975). *La perspective comme forme symbolique*. Les éditions de Minuit.

J. PEONIS, J. WINEMAN, M. RASCHID, S. H. KIM, and S. BAFNA (1997). On the description of shape and spatial configuration inside buildings: convex partitions and their local properties. *Environment and Planning B: Planning and Design*, 24(5):761–781.

S. PETITJEAN (1996). The enumerative geometry of projective algebraic surfaces and the complexity of aspect graphs. *International Journal of Computer Vision*, 19(3):1–27, 1996.

H. PLANTINGA and C. R. DYER (1990). Visibility, occlusion, and the aspect graph. *International Journal of Computer Vision*, 5(2):137–160.

C. R. V. TANDY (1967). *The isovist method of landscape survey*. Ed. H. C. Murray (Landscape Research Group, London).

J. TELLER (2001). *La régulation morphologique dans le cadre du projet urbain : Spécification d'instruments informatiques destinés à supporter les modes de régulation performantiels*. PhD thesis, Université de Liège.

J. TELLER and S. AZAR (2001). Townscope II – A computer system to support solar access decisionmaking. *Solar Energy Journal*, 70(3):187–200.

P. THIEL (1969). La notation de l'espace, du mouvement et de l'orientation. *Architecture d'Aujourd'hui*, 145:49–58.

A. TURNER (2001). Depthmap: A program to perform visibility graph analysis. In *Proceedings of the 3rd Symposium on Space Syntax*, Georgia Institute of Technology.

A. TURNER, M. DOXA, D. O'SULLIVAN, and A. PENN (2001). From isovists to visibility graphs: a methodology for the analysis of architectural space. *Environment and Planning B: Planning and Design*, 28(1):103–121.

A. TURNER and A. PENN (1999). Making isovists syntactic: isovist integration analysis. In *Proceedings of the 2nd Symposium on Space Syntax*, Universidad de Brasilia, Brazil.

E. W. WEISSTEIN (1999). *Concise Encyclopedia of Mathematics CD-ROM*. Chapman & Hall/CRCnetBASE. [CD-ROM] edition 1.0.

J. A. WISE (1985). The quantitative modelling of human spatial habitability. Technical Report NAG 2–346, NASA.